Supplemental Information

Novel high performance poly(p-phenylene benzobisimidazole) (PBDI) membranes fabricated by interfacial polymerization for H_2 separation

Meixia Shan[a], Xinlei Liu[a*], Xuerui Wang[a], Zilong Liu[b], Hodayfa Iziyi[a], Swapna Ganapathy[c], Jorge Gascon[a,d] and Freek Kapteijn[a*]

[a] Catalysis Engineering, Chemical Engineering Department, Delft University of Technology, Van der Maasweg, 9, 2629 HZ Delft, The Netherlands
Emails: x.liu-8@tudelft.nl; f.kapteijn@tudelft.nl

[b] Organic Materials & Interface, Chemical Engineering, Delft University of Technology, Van der Maasweg 9, 2629 HZ Delft, The Netherlands

[c] Department of Radiation Science and Technology, Delft University of Technology, Mekelweg 15, 2629 JB Delft, The Netherlands

[d] King Abdullah University of Science and Technology, KAUST Catalysis Center, Advanced Catalytic Materials. Thuwal 23955, Saudi Arabia

Movie S1. As attached, a free standing PBDI film was prepared by spreading the terephthalaldehyde (TPA) toluene solution on top of the 1,2,4,5-benzenetetramine tetrahydrochloride (BTA) aqueous solution. A strong thin film formed at the interface.

Table S1. Performance of PBDI membranes with different reaction duration in the separation of H_2 from an equimolar mixture of H_2 and CO_2 at 1 bara, 373 K, and He sweep gas. M1-2, M2-2 and M3-2 are duplicates of M1-1, M2-1 and M3-1, respectively.

| Membranes	Reaction time / h	Membrane performance		
		H_2 Permeance (GPU)	CO_2 Permeance (GPU)	H_2/CO_2 selectivity
M1-1	1	86.9	4.72	18.4
M1-2	1	68.2	4.01	17.0
M2-1	2	123	5.69	21.6
M2-2	2	114	4.81	23.7
M3-1	3	78.0	3.84	20.3
M3-2	3	64.6	3.03	21.3

The Virial equation [1,2] (Eq. *(S1)* and *(S2)*) was used to calculate the steric heat of adsorption Q_{st} as a function of loading. In these equations p is the absolute pressure in mmHg, T is the temperature in K, n is the adsorbed amount in mg·g^{-1}, R is the ideal gas constant in J·K^{-1} mol^{-1} and a, b are estimated fitting parameters from the combined adsorption isotherms. Only parameters a_0, a_1, a_2 and b_0 were significant in this case.

$$\ln(p) = \ln(n) + \frac{1}{T}\sum_{i=0}^{2} a_i n^i + b_0$$

(S1)

$$Q_{st} = -R\sum_{i=0}^{2} a_i n^i$$

(S2)

Table S2. Fitted Parameters in Virial equation (*S1*).

| Parameters	Value	Standard deviation
a_0	-4199	60.5
a_1	38.99	2.79
a_2	-0.5497	0.145
b_0	17.16	0.193

3
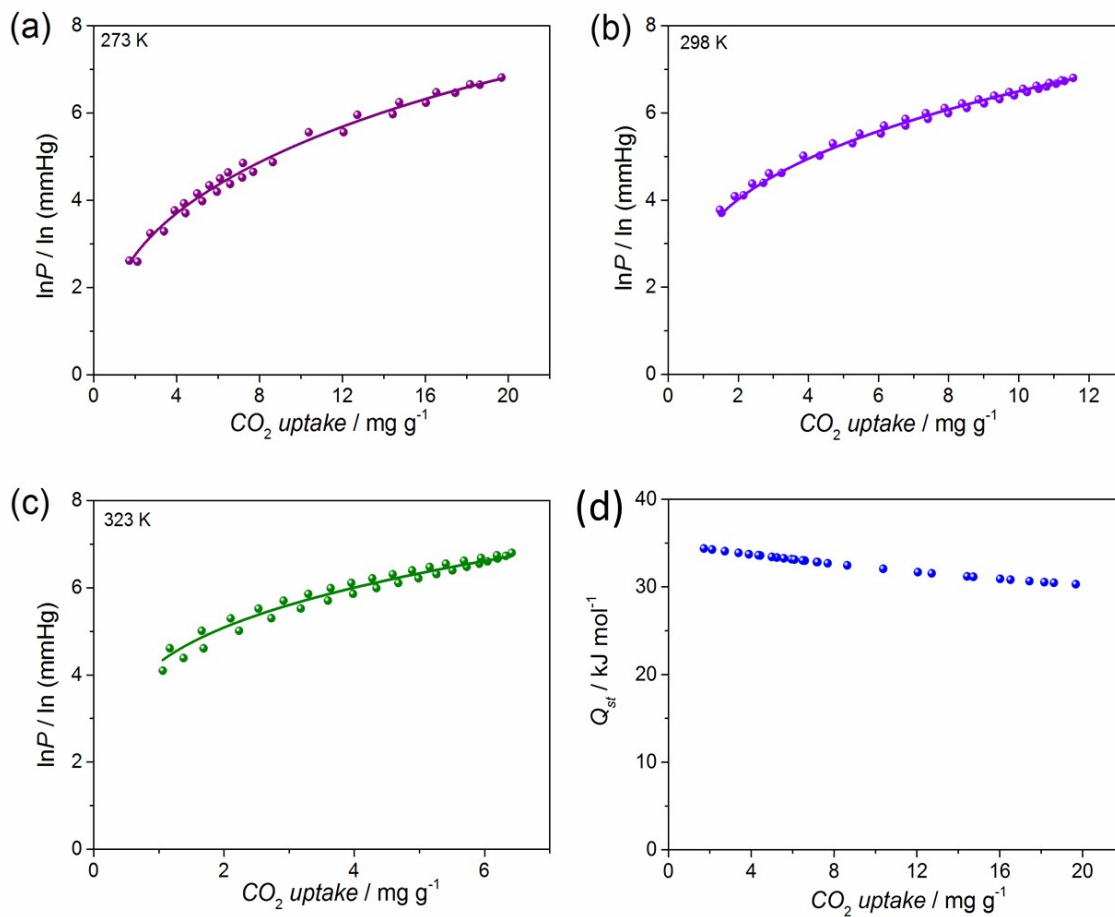
Fig. S1. Experimental data and Virial equation fit for CO_2 adsorption-desorption isotherms of PBDI films at (a) 273 K, (b) 298 K and (c) 323 K, respectively (Fig. 3f). (d) CO_2 isosteric heat of adsorption on PBDI films as a function of loading calculated with the Virial equation parameters in Table S2.
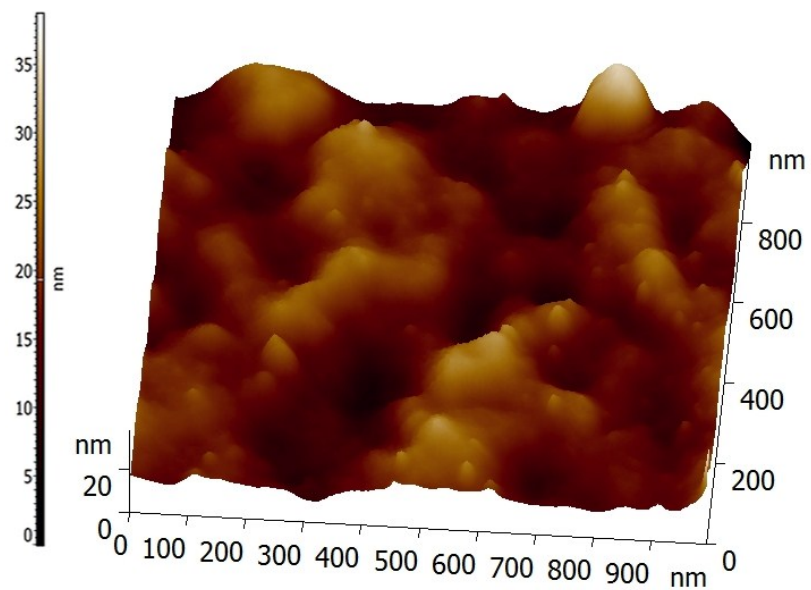
Fig. S2. 3D AFM image of PBDI membrane surface (M2-1) corresponding to the 2D AFM image of Fig. 4b. Particles with size down to 20 nm were possibly recognized on the membrane surface.
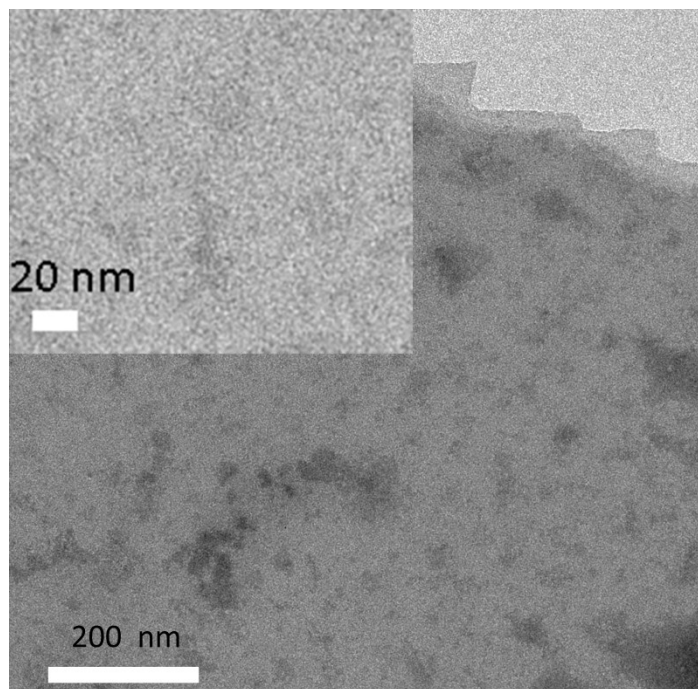
Fig. S3. High-resolution TEM images of PBDI film.

Transmission electron microscopy (TEM) test was performed on a JEOL JEM1400 plus operated at 120 kV. The specimens were prepared by applying a few drops of the PBDI film ethanol suspensions on a carbon-coated copper grid and letting it dry.
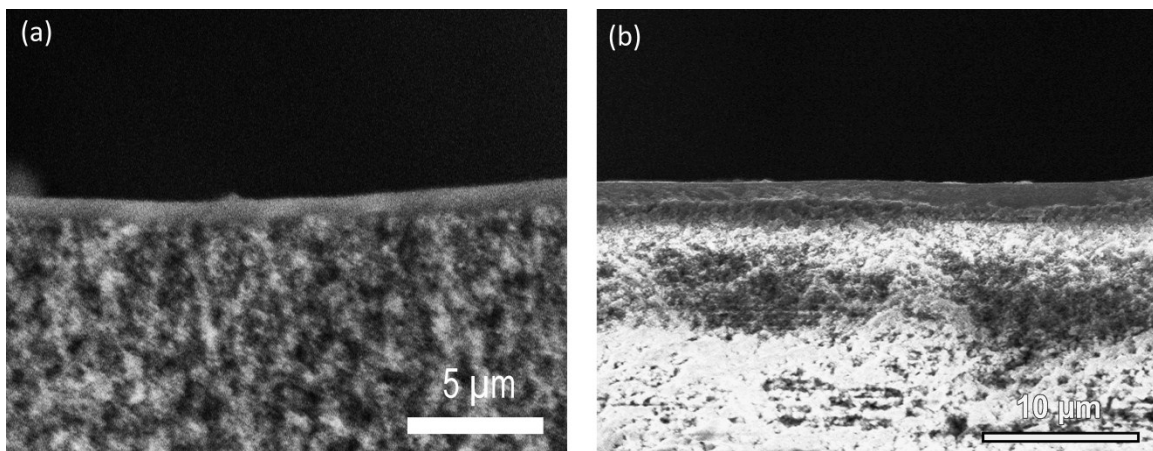
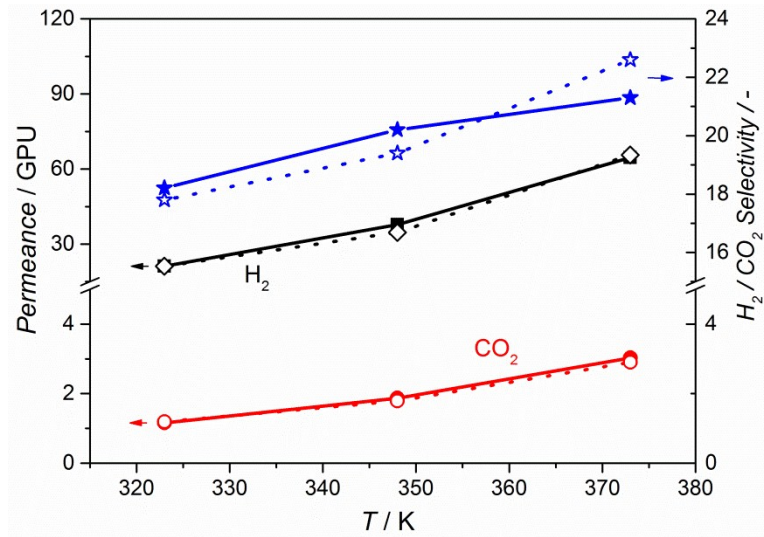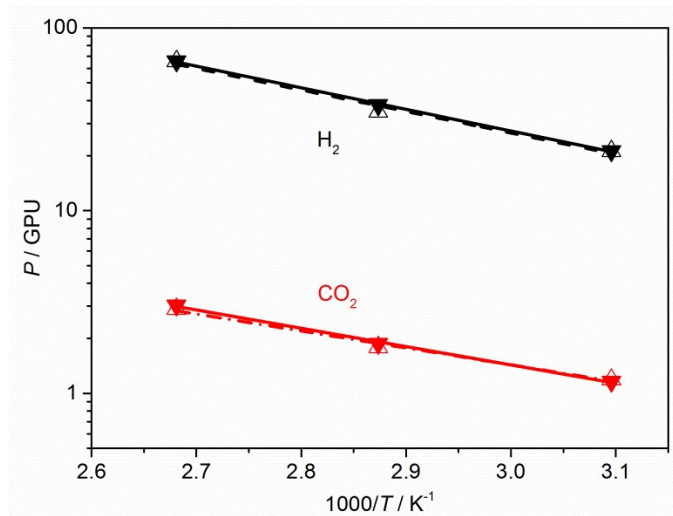**Fig. S4.** Cross-sectional SEM images of (a) M1-1 and (b) M3-1 membranes. The membrane thickness is ca. 0.6 and 1.3 μm, respectively.

Fig. S5. Effect of the temperature on the membrane separation performance for membrane M3-2 at 1 bara. Dashed and solid lines correspond to single component and equimolar mixed gas feed, respectively. Helium was used as sweep gas.

Fig. S6. Arrhenius temperature dependence of H_2 and CO_2 permeances for the PBDI membrane (M3-2) at 1 bara feed pressure. Dashed and solid lines correspond to single component and equimolar mixed gas feed, respectively (data of Fig. S5).

The permeance of each gas was correlated with the temperature through the Van't Hoff-Arrhenius equation:

$$P_i = A_i * exp\left(-\frac{E_{act,i}}{R * T} \right),$$

(S3)

so,

$$ln(P_i) = a - (\frac{E_{act,i}}{R}) * (\frac{1}{T})$$

where P_i is the permeance of component i, A_i represents for the pre-exponential factor of component i, $E_{act,i}$ is the apparent activation energy of component i, R is the ideal gas constant (8.314 J mol^{-1} K^{-1}) and T is the absolute temperature (K). A plot of ln (P_i) versus (1/T) was given together with a linear fitting (Fig. S6). The temperature dependency of the permeation flux is found to follow an Arrhenius type of relation for both the single and mixed gas test. The apparent activation energies for H_2 and CO_2 permeation are listed in Table S2. There is not much difference between the component permeances in the single component and mixed gas permeation processes, indicating the weak competitive permeation. In all cases, the apparent activation energy for H_2 permeation is higher than that of CO_2, indicating H_2 permeation is more sensitive with temperature, leading to an increase in the H_2/CO_2 selectivity as the temperature increased (Fig. S5). The lower apparent permeation activation energy of CO_2 is attributed to the lowering contribution of the (negative) adsorption enthalpy. At the low adsorption loadings the diffusivity activation energy of CO_2 can be calculated with equation S5:

$$E_{diff} = E_{act} + Q_{St}$$

(S5)

The value is 52.2 kJ mol^{-1}, demonstrating activated diffusion for CO_2.

Table S3. Permeance at different temperatures, fitting parameters of Fig. S6 and activation energies for the permeation of single and mixed gases in PBDI (M3-2) membrane at 1 bara.

	Permeance / GPU			Fitting parameters		$E_{act,I}$ /	Q_{st} /	E_{diff} /
				Intercept	Slope	kJ mol^{-1}	kJ mol^{-1}	kJ mol^{-1}
	323 K	348 K	373 K	(a)	($-E_{act,i}$/R)			
Single H_2	21.2	34.7	65.7	-10.4	-2.72	22.6	-	
Mixed H_2	21.2	37.8	64.6	-10.4	-2.68	22.3		
Single CO_2	1.19	1.79	2.90	-15.0	-2.14	17.8	34.4	52.2
Mixed CO_2	1.16	1.87	3.03	-14.5	-2.31	19.2		
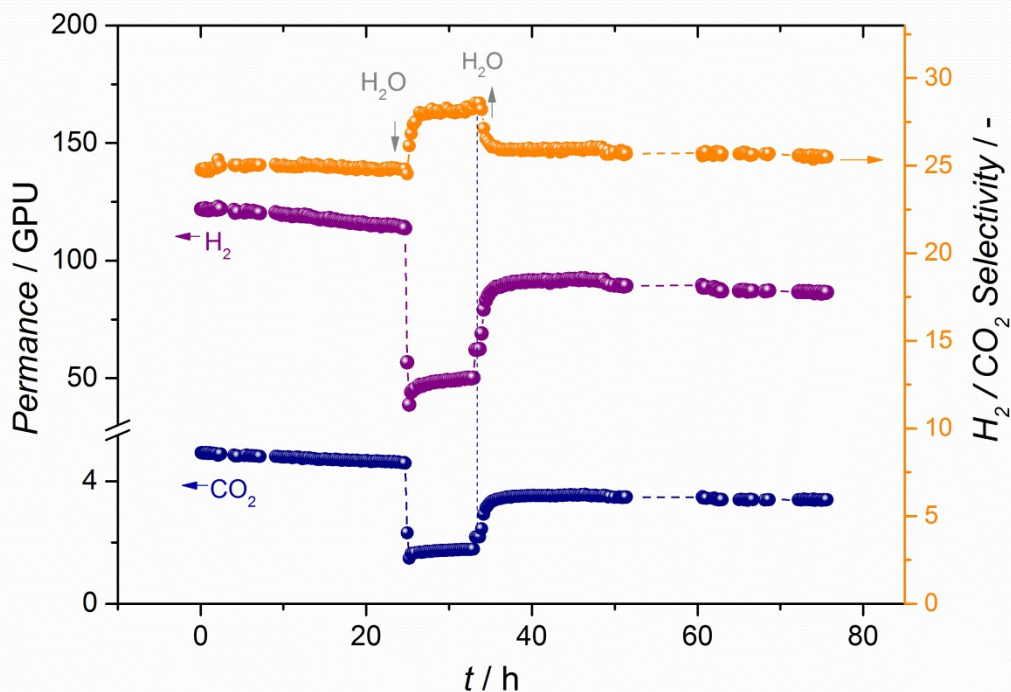
Fig. S7. Stability test of M2-1 for mixed H_2/CO_2 separation under alternating dry and wet gas mixtures (2.3 mol.% H_2O) at 373 K and 1 bara.

As shown in Fig. S7, the M2 membrane exhibited a good stability. Originally, both H_2 and CO_2 permeance showed a slow decrease. Nevertheless, after the water exposure this decline was stopped. So, water probably rearranged the polymer chains and stabilized the packing. Both H_2 and CO_2 permeance decreased when 2.3 mol.% H_2O was introduced in the feed, attributed to the adsorption of H_2O molecules that narrowed the pathways of penetrants and decreased the polymer chain spacing because of hydrogen bonding,[3] which increases the diffusion resistance for both gases. Such resistance has a more significant effect on the bigger CO_2 molecules resulting in an increased H_2/CO_2 selectivity under wet conditions.

9

Table S4. Comparison of the performance of the as-synthesized PBDI membranes with reported PBI-related membranes. Permeance with the unit of GPU and selectivity were collected. The data above and below the dashed line are from PBI and modified PBI membranes, respectively. 1 GPU = 3.35×10^{-10} mol m^{-2} s^{-1} Pa^{-1}.

Membrane material	Performance			Operation conditions		Reference
	P_{H2} (GPU)	H$_2$/CO$_2$ selectivity (-)	Type of analysis	Feed temperature T/ K	Feed pressure p (bara)	
PBI	0.33	7.89	Single gas	373	5-8	4
	0.64	13.62	Single gas	473	5-8	
	0.99	21.74	Single gas	573	5-8	
	2.60	27.28	Single gas	673	5-8	
	3.564	23.03	Single gas	523	3.4	5
	50-500	17-25	Single gas	523-623	NA	6
	50	24	Single gas	523-623	NA	
	530	18	Single gas	523-623	NA	
	0.086	5.2	Single gas	333	1	7
PBI-PDMS	6.5	12.6	Mixed gas	453	3	8
	20.3	35.6	Mixed gas	523	6	
PBI-Matrimid	38.67	6.85	Single gas	308	3.5	9
PBI-Matrimid-PDMS	29.26	11.11	Single gas	308	3.5	
PBI composite	1.6	58	Single gas	423	3.4	10
	3	49	Single gas	473	3.4	
	4.67	43	Single gas	523	3.4	
	7	47	Mixed gas	523	3.4	
BILP-101x	24.2	39.5	Mixed gas	423	2	11
	36.4	34.2	Mixed gas	423	1	
PBDI (M2-1)	241	22.7	Mixed gas	423	1	This work
PBDI (M3-1)	182	22.2	Mixed gas	423	1	

Table S5. Comparison of the performance of the as-synthesized PBDI membranes with reported PBI-related membranes. Permeability with the unit of Barrer and selectivity were collected. The data above and below the dashed line are from PBI and modified PBI membranes, respectively. 1 Barrer = 3.35×10^{-16} mol m m^{-2} s^{-1} Pa^{-1}.

Membrane material	Performance			Operation conditions		Reference
	P_{H2} (Barrer)	H$_2$/CO$_2$ *selectivity* (-)	Type of analysis	Feed temperature T (K)	Feed pressure p (bara)	
PBI	0.09	9	Single gas	298	3.4	12
PBI	11	3.7	Mixed gases	593	3.4	
PBI	76.8	23.0	Single gas	523	3.4	5
PBI	26	16	Single gas	423	8-15	13
PBI	10	11	Mixed gas	373	11	
PBI	25	11	Mixed gas	423	11	14
PBI	40	12	Mixed gas	473	11	
PBI	45.5	1.4	Single gas	423	5	15
PBI	77.4	4.1	Single gas	473	5	
PBI	30	3.8	Mixed gas	423	6	16
PBI	3.5	9	Single gas	308	5	17
PBI	17.2	5	Single gas	RT	NA	18
PBI	3.7	8.6	Single gas	308	3.5	19
PBI	2.9	7.1	Mixed gas	308	7	20
PBI	70	8.2	Mixed gas	453	7	
PBI	2.9	7.1	Mixed gas	308k	2	21
PBI	55	3.5	Mixed gas	453	2	22
PBI-HFA	200	3.2	Single gas	373	8	
PBI-HFA	250	4.5	Single gas	423	8	23
PBI-HFA	310	5.4	Single gas	473	8	
TADPS-IPA PBI	3.6	32	Single gas	308	10	24
PBI-H3PO4-0.16	12	34	Mixed gas	423	14	13
PBI-H3PO4-1.0	1.5	140	Single gas	423	8-15	
PBI-PPC	5.0	14.4	Single gas	308	10	6

PBI-g-PEO	6.9	10.5	Single gas	308	10	25
50PBI-0.7DBX-300	46.2	9.9	Mixed gas	423	7	26
XLPBI-6H	8.6	18	Mixed gas	373	11	
XLPBI-6H	19	18	Mixed gas	423	11	14
XLPBI-6H	38	17	Mixed gas	473	11	
PBI-HFA	276	4.5	Single gas	423	8	27
50/50: 6F/m-PBI	110	4	Single gas	373	3.4	
50/50: 6F/m-PBI	150	6	Single gas	423	3.4	28
50/50: 6F/m-PBI	240	7	Single gas	473	3.4	
50/50: 6F/m-PBI	360	7.3	Single gas	523	3.4	
PBI-BuI	10.7	5.6	Single gas	308	20	29
FDD-PBI	4.04	40.4	Single gas	308	2.7	30
PBI-Matrimid	3.6	26.1	Single gas	308	3.5	31
PBDI (M2-1)	193	22.7	Mixed gas	423	1	This work
PBDI (M3-1)	146	22.2	Mixed gas	423	1	This work

References

1. M. S. Sun, D. B. Shah, H. H. Xu and O. Talu, *The Journal of Physical Chemistry B*, 1998, 102, 1466-1473.
2. L. Czepirski and J. Jagiełło, *Chemical Engineering Science*, 1989, 44, 797-801.
3. S. Li, J. R. Fried, J. Colebrook and J. Burkhardt, *Polymer*, 2010, 51, 5640-5648.
4. S. C. Kumbharkar, Y. Liu and K. Li, *Journal of Membrane Science*, 2011, 375, 231-240.
5. X. Li, R. P. Singh, K. W. Dudeck, K. A. Berchtold and B. C. Benicewicz, *Journal of Membrane Science*, 2014, 461, 59-68.
6. R. P. Singh, G. J. Dahe, K. W. Dudeck, C. F. Welch and K. A. Berchtold, *Energy Procedia*, 2014, 63, 153-159.
7. L. F. Villalobos, R. Hilke, F. H. Akhtar and K.-V. Peinemann, *Advanced Energy Materials*, 2018, 8, 1701567.
8. J. Sánchez-Laínez, B. Zornoza, C. Téllez and J. Coronas, *Journal of Membrane Science*, 2018, 563, 427-434.
9. S. S. Hosseini, N. Peng and T. S. Chung, *Journal of Membrane Science*, 2010, 349, 156-166.
10. K. A. Berchtold, R. P. Singh, J. S. Young and K. W. Dudeck, *Journal of Membrane Science*, 2012, 415-416, 265-270.
11. M. Shan, X. Liu, X. Wang, I. Yarulina, B. Seoane, F. Kapteijn and J. Gascon, *Science Advances*, 2018, 4, eaau1698.
12. D. R. Pesiri, B. Jorgensen and R. C. Dye, *Journal of Membrane Science*, 2003, 218, 11-18.
13. L. Zhu, M. T. Swihart and H. Lin, *Energy & Environmental Science*, 2018, 11, 94-100.
14. L. Zhu, M. T. Swihart and H. Lin, *Journal of Materials Chemistry A*, 2017, 5, 19914-19923.
15. H. S. M. Suhaimi, C. P. Leo and A. L. Ahmad, *Chemical Engineering & Technology*, 2017, 40, 631-638.
16. J. Sánchez-Laínez, B. Zornoza, S. Friebe, J. Caro, S. Cao, A. Sabetghadam, B. Seoane, J. Gascon, F. Kapteijn, C. Le Guillouzer, G. Clet, M. Daturi, C. Téllez and J. Coronas, *Journal of Membrane Science*, 2016, 515, 45-53.
17. Z. Kang, Y. Peng, Y. Qian, D. Yuan, M. A. Addicoat, T. Heine, Z. Hu, L. Tee, Z. Guo and D. Zhao, *Chemistry of Materials*, 2016, 28, 1277-1285.
18. L. Li, J. Yao, X. Wang, Y.-B. Cheng and H. Wang, *Journal of Applied Polymer Science*, 2014, 131.
19. T. Yang, G. M. Shi and T.-S. Chung, *Advanced Energy Materials*, 2012, 2, 1358-1367.

20.   T. Yang, Y. Xiao and T.-S. Chung, *Energy & Environmental Science*, 2011, 4, 4171-4180.
21.   T. Yang and T.-S. Chung, *International Journal of Hydrogen Energy*, 2013, 38, 229-239.
22.   J. Sánchez-Laínez, B. Zornoza, C. Téllez and J. Coronas, *Journal of Materials Chemistry A*, 2016, 4, 14334-14341.
23.   S. H. Choi, D. H. Kim, D. Y. Kim, J. Y. Han, C. W. Yoon, H. C. Ham, J.-H. Kim, H.-J. Kim, S. W. Nam, T.-H. Lim and J. Han, *Journal of Applied Polymer Science*, 2015, 132, 42371.
24.   H. Borjigin, K. A. Stevens, R. Liu, J. D. Moon, A. T. Shaver, S. Swinnea, B. D. Freeman, J. S. Riffle and J. E. McGrath, *Polymer*, 2015, 71, 135-142.
25.   R. M. Joseph, M. M. Merrick, R. Liu, A. C. Fraser, J. D. Moon, S. R. Choudhury, J. Lesko, B. D. Freeman and J. S. Riffle, *Journal of Membrane Science*, 2018, 564, 587-597.
26.   N. Akbar and C. Martin, *Journal of membrane science*, 2018, 563, 726-733.
27.   S. Y. Kong, D. H. Kim, D. Henkensmeier, H.-J. Kim, H. C. Ham, J. Han, S. P. Yoon, C. W. Yoon and S. H. Choi, *Separation and Purification Technology*, 2017, 179, 486-493.
28.   R. P. Singh, X. Li, K. W. Dudeck, B. C. Benicewicz and K. A. Berchtold, *Polymer*, 2017, 119, 134-141.
29.   S. C. Kumbharkar, P. B. Karadkar and U. K. Kharul, *Journal of Membrane Science*, 2006, 286, 161-169.
30.   N. P. Panapitiya, S. N. Wijenayake, D. D. Nguyen, Y. Huang, I. H. Musselman, K. J. Balkus and J. P. Ferraris, *ACS Applied Materials & Interfaces*, 2015, 7, 18618-18627.
31.   S. S. Hosseini, M. M. Teoh and T. S. Chung, *Polymer*, 2008, 49, 1594-1603.